Support effects in the selective gas phase hydrogenation of *p*-chloronitrobenzene over gold

Fernando Cárdenas-Lizana, Santiago Gómez-Quero, Noémie Perret and Mark A. Keane*

Chemical Engineering,
School of Engineering and Physical Sciences,
Heriot-Watt University, Edinburgh EH14 4AS, Scotland

* Corresponding author: Tel: +44(0)131 451 4719
E-mail: M.A.Keane@hw.ac.uk

Abstract

The catalytic continuous gas phase hydrogenation of *p*-chloronitrobenzene (*P* = 1 atm; *T* = 423 K) has been investigated over a series of oxide (Al_2O_3, TiO_2, Fe_2O_3 and CeO_2) supported Au (1 mol %) catalysts. The application of two catalyst synthesis routes, *i.e.* impregnation (IMP) and deposition-precipitation (DP), has been considered where the DP route generated smaller mean Au particle sizes (1.5-2.8 nm) compared with the IMP preparation (3.5-9.0 nm). The catalysts have been characterised in terms H_2 chemisorption and BET area measurements where the formation of metallic Au post-activation has been verified by diffuse reflectance UV-Vis, XRD and HRTEM analyses. *p*-Chloroaniline was generated as the sole reaction product over all the Au catalysts with no evidence of C-Cl and/or C-NO_2 bond scission and/or aromatic ring reduction. The specific hydrogenation rate increased with decreasing Au particle size (from 9 to 3 nm), regardless of the nature of the support. This response extends to a reference Au/TiO_2 catalyst provided by the World Gold Council. A decrease in specific rate is in evidence for smaller particles (< 2 nm) and can be attributed to a quantum size effect. The results presented establish the basis for the design and development of a versatile catalytic system for the clean continuous production of high value amino compounds under mild reaction conditions.

Keywords: Gold catalysts; *p*-chloronitrobenzene hydrogenation; *p*-chloroaniline; Au particle size; catalyst support effect

Introduction

Hydrogenation promoted by gold has emerged as one of the most challenging topics in gold catalysis, as reflected in the reviews by Claus [1] and Hashmi [2]. The lower hydrogenation activity associated with Au when compared with traditional metals (*e.g.* Pt, Pd) [3,4] is compensated for in terms of the high selectivity that Au can deliver in hydrogenation applications [1]. In order to develop viable processes based on Au catalysis, an explicit correlation of activity/selectivity with catalyst structure is required. One issue that must be resolved is the difference in catalytic performance observed for Au supported on different oxide carriers [1,3,5-9]. The nature of the support can affect the morphology and dispersion of Au particles via metal-support interactions [3,10,11] and it is established that smaller (≤ 10 nm) supported Au particles exhibit electronic properties that are quite distinct from bulk Au [12]. This feature is critical in that the catalytic response of Au in hydrogenation reactions may be dependent on changes in the electronic character of the supported metal [13]. Furthermore, while the carrier can impact on the properties of the Au component, the supported Au phase has been reported to induce changes in the oxide support, notably by promoting the reduction of (reducible) oxides, including Fe_2O_3 [14], CeO_2 [15] and TiO_2 [16,17]. Considering the complex nature of Au-support interactions, it is not surprising that the effect of the support on the hydrogenation response still remains largely unresolved.

The selective reduction of aromatic nitro-group substituents in the presence of other functional groups (*e.g.* carbonyl, cyano, chloro or alkenic groups) is difficult as the reduction/substitution of these groups (by H_2) can be more facile than the target -NO_2 group [18,19]. In the selective reduction of nitroarenes, promising results have been recently published for supported gold catalysts in batch liquid operation [20-26], although the formation of highly toxic by-products (azoxy-derivates) and the requirement of high hydrogen pressures (3-4 MPa) are drawbacks that require further consideration. *p*-Chloroaniline (the target product in this study) is a high production volume compound [27] extensively used as an intermediate in the synthesis of a broad range of fine chemicals, *e.g.* pharmaceuticals and agrochemicals [28]. The traditional production route from *p*-chloronitrobenzene involves the use of Fe in acid media (Béchamp process) but the generation of large amounts (5-20 times greater than that of the target product) of toxic waste (Fe hydroxide sludge) and low overall product yields have limited its applicability [29]. Catalytic hydrogenation in batch liquid systems over transition metal catalysts provides a cleaner alternative [30]. However, the challenge is to achieve

Figure 1

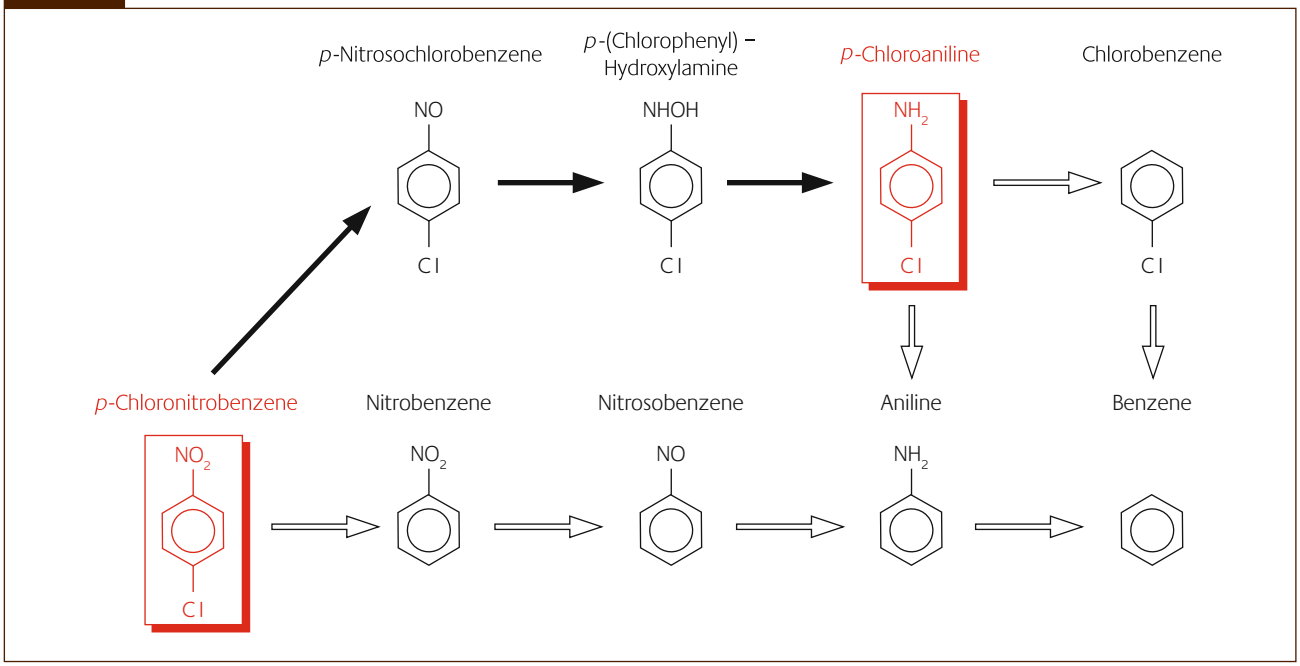

Reaction pathways associated with the hydrogen mediated conversion of p-chloronitrobenzene. Note: Targeted route to p-chloroaniline is represented by bold arrows. The p-chloronitrobenzene reactant and p-chloroaniline product are framed in red

selective hydrogenation of the nitro group and avoid scission of the C-Cl bond [30,31] and/or cleavage of -NH_2 [32] from the product. The hydrogenolysis of the Cl substituent can lead to the formation of aniline either (a) via the reduction of nitrobenzene or (b) as a result of the further transformation of *p*-chloroaniline as shown in Figure 1, with both steps reported in the literature for catalytic operation (in gas and/or liquid phase) over supported metals [32-40].

We have recently demonstrated exclusivity in the hydrogenation of a series of halonitrocompounds to the respective halogenated aromatic amine in continuous gas phase operation over supported Ni [41] and Au [33,42]. In those studies, we recorded a higher catalytic activity for the Ni catalysts but significant time on-stream deactivation was in evidence. In this contribution, we have extended that work to probe the effect of the support in modifying the catalytic action of a well dispersed Au phase. We have considered four oxide supports (Al_2O_3, TiO_2, CeO_2 and Fe_2O_3) that present a range of acid-base and redox surface properties. In addition, we have compared the catalytic behaviour of these systems with a Au/TiO_2 reference catalyst supplied by the World Gold Council.

Experimental

Catalyst preparation and activation

The effect of the support on Au catalytic hydrogenation performance was investigated by selecting a group of reducible (CeO_2, TiO_2 and α-Fe_2O_3) and non-reducible (γ-Al_2O_3) oxides. The CeO_2 (HSA5, Rhodia), TiO_2 (P25, Degussa) and γ-Al_2O_3 (Puralox, Condea Vista Co.) supports were used as received. Hematite (α-Fe_2O_3) was prepared by precipitation in basic media according to [43-45]

$$2[Fe(NO_3)_3 9H_2O] + 3Na_2CO_3 \rightarrow 2Fe(OH)_3 + 6NaNO_3 + 3CO_2 + 15H_2O \quad (1)$$

100 cm^3 aqueous Na_2CO_3 (1 M) were placed in a three-necked round-bottom flask and heated in a water bath to 358±5 K under constant agitation (300 rpm). An aqueous solution of $Fe(NO_3)_3 \cdot 9H_2O$ (300 cm^3, 1 M) was then added drop wise (300 cm^3 h^{-1}) by means of a microprocessor-controlled infusion pump (100 kd Scientific). Basic conditions (pH > 7.3) were maintained during precipitation by adding Na_2CO_3 (five additions of 10g). The solid hydroxide was subsequently aged for 2 h to enhance the BET area [45], washed with warm distilled water until the wash water approached neutral pH and dried for 3 days at 353 K (2 K min^{-1}) in ultra pure He (60 cm^3 min^{-1}) to produce hematite:

$$2Fe(OH)_3 \rightarrow Fe_2O_3 + 3H_2O \quad (2)$$

The X-ray diffractogram pattern for the as prepared Fe_2O_3 (not shown) presented signals at 2θ = 24.1°, 33.2°, 35.6°, 40.9°, 49.5°, 54.1°, 57.6°, 62.4° and 64.0° corresponding to the (012), (104), (110), (113), (024), (116), (018), (214) and (300) characteristics planes of α-phase Fe_2O_3 (hematite, JCPDS-ICDD card number 33-0664). A series of 1 mol % oxide supported Au was prepared by deposition-precipitation (DP) and impregnation (IMP). These synthesis routes were chosen as it has been demonstrated that catalyst synthesis can

significantly influence metal dispersion where DP has been shown to generate small Au particles (< 5 nm) (46,47). In contrast, even at low Au loading (1-2 wt. %), catalysts prepared by the less controlled IMP procedure normally exhibit larger (10-35 nm) Au diameters (5). In the case of the DP samples, urea (used as the basification agent) was added (ca. 100-fold urea excess) to a solution of $HAuCl_4$ (300 cm^3, 5 x 10^{-4} M). The support (3-5 g, γ-Al_2O_3, TiO_2, CeO_2 and α-Fe_2O_3) was introduced and the suspension was stirred and heated to 353 K for 16 h. The pH of the suspension progressively increased to reach ca. 7 after 16 h as a result of the thermally-induced urea decomposition [48]

$$NH_2\text{-}CO\text{-}NH_2 + 3H_2O \xrightarrow{T=353K} 2NH_4^+ + 2OH^- + CO_2 \quad (3)$$

The solids obtained were separated by centrifugation, washed three times with deionized water and dried under vacuum at 298 K for 12 h. In the case of the IMP synthesis, the support was dispersed in appropriate volumes of $HAuCl_4$ solution (Aldrich, 25 x 10^{-3} g cm^{-3}, pH = 2) and the resulting slurry was vigorously stirred (600 rpm) and heated (2 K min^{-1}) to 353 K in a He purge. The solid residue was dried in a flow of He at 383 K for 3 h. After preparation, the samples were sieved to 75 μm average particle diameter and stored (in the dark) at 298 K. The Au loading was determined (to within ±2 %) by inductively coupled plasma-optical emission spectrometry (ICP-OES, Vista-PRO, Varian Inc.) from the diluted extract of aqua regia. The catalytic behaviour of a 1 mol % Au/TiO_2 reference catalyst supplied by the World Gold Council (type A, lot number Au-TiO_2 #02-7, sample number 110) was also investigated. The preparation and characterization details of this reference sample have been recorded elsewhere [49,50]. Prior to use in catalysis, the samples were activated in 60 cm^3 min^{-1} H_2 at 2 K min^{-1} to 423-603±1 K and maintained at final reduction temperature for 1 h. The requirements for the reduction of the Au precursor to metallic Au for catalysts prepared by IMP and/or DP have been established elsewhere [33,42,51]. Samples for off-line analysis were passivated in 1% v/v O_2/He at room temperature.

Catalyst characterization

H_2 chemisorption and BET surface area were determined using the commercial CHEM-BET 3000 (Quantachrome) unit. The samples were activated as above, swept with a 65 cm^3 min^{-1} flow of N_2 for 1.5 h, cooled to room temperature and subjected to H_2 chemisorption using a pulse (10 μl) titration procedure. BET areas were recorded with a 30% v/v N_2/He flow using pure N_2 (99.9%) as internal standard. At least 2 cycles of N_2 adsorption-desorption in the flow mode were employed to determine total surface area using the standard single point method. BET surface area and H_2 uptake values were reproducible to within ±5%. Powder X-ray diffractograms were recorded on a Bruker/Siemens D500 incident X-ray diffractometer using Cu Kα radiation. The samples were scanned at 0.02° $step^{-1}$ over 20° ≤ 2θ ≤ 90° (scan time = 5 s $step^{-1}$). Diffractograms were identified using the JCPDS-ICDD reference standards, *i.e.* γ-Al_2O_3 (10-0425) and Au (4-0784). Diffuse reflectance (DRS UV-Vis) measurements were conducted using a Perkin Elmer Lambda 35 UV-Vis Spectrometer with $BaSO_4$ powder as reference; absorption profiles were calculated from the reflectance data using the Kubelka-Munk function. Au particle morphology and size were determined by transmission electron microscopy analysis; JEOL JEM 2011 HRTEM unit with a UTW energy dispersive X-ray detector (Oxford Instruments) operated at an accelerating voltage of 200 kV. Specimens were prepared by dispersion in acetone and deposited on a *holey* carbon/Cu grid (300 Mesh). Up to 1000 individual Au particles were counted for each catalyst and the surface area-weighted metal diameter (d_{TEM}) was calculated from

$$d_{TEM} = \frac{\sum_i n_i d_i^3}{\sum_i n_i d_i^2} \quad (4)$$

where n_i is the number of particles of diameter d_i. The size limit for the detection of Au particles is *ca.* 1 nm.

Catalysis procedure

Reactions were carried out under atmospheric pressure at T = 423 K, in situ immediately after activation, in a fixed bed vertical plug-flow glass reactor (l = 600 mm; i.d. = 15 mm). The catalytic reactor and operating conditions to ensure negligible heat/mass transport limitations, have been fully described elsewhere [52] but some features, pertinent to this study, are given below. A layer of borosilicate glass beads served as preheating zone, ensuring that the *p*-chloronitrobenzene reactant was vaporized and reached reaction temperature before contacting the catalyst. Isothermal conditions (±1 K) were ensured by diluting the catalyst bed with ground glass (75 μm) [53]. The reactant was delivered to the reactor via a glass/teflon air-tight syringe and teflon line using a microprocessor controlled infusion pump (Model 100 kd Scientific) at a fixed calibrated flow rate. A co-current flow of *p*-chloronitrobenzene and ultra pure H_2 (< 1% v/v -NO_2/H_2) was maintained at a $GHSV$ = 2 x 10^4 h^{-1} with an inlet -NO_2 molar flow (F) in the range 15x10^{-2} – 38x10^{-2} mmol$_{\text{-}NO_2}$ h^{-1}, where the H_2 content was up to 350 times in excess of the stoichiometric requirement (P_{H_2}= 0.92 atm), the flow rate of which was monitored using a Humonics (Model 520) digital flowmeter. The molar metal (n_{Au}) to inlet molar -NO_2 feed rate (F) ratio spanned the range 5x10^{-4}–169x10^{-4} h. In a series of blank tests, passage of *p*-chloronitrobenzene in a stream of H_2 through the empty reactor or over the support alone, *i.e.* in the absence Au, did not result in any detectable conversion. The reactor effluent was frozen in a liquid nitrogen trap for subsequent analysis, which was made using a Perkin-Elmer Auto System XL gas chromatograph equipped with a programmed split/splitless injector and a flame ionization

detector, employing a DB-1 50 m x 0.20 mm i.d., 0.33 µm film thickness capillary column (J&W Scientific), as described elsewhere [54]. Any possible HCl produced was monitored by passing the effluent gas through an aqueous NaOH trap (7.0×10^{-4} mol dm^{-3}, kept under constant agitation at 400 rpm) with continuous pH (Hanna HI Programmable Printing pH Bench-Meter) analysis. *p*-Chloronitrobenzene (Aldrich, ≥99.9% w/w purity) and the *1*-butanol solvent (Riedel-de Häen, ≥ 99.5 %) were used without further purification. Hydrogenation performance is quantified in terms of the degree of nitro-group reduction (x_{-NO_2})

$$x_{-NO_2} = \frac{[-NH_2]_{out}}{[-NO_2]_{in}} \quad (5)$$

The percentage selectivity with respect to *p*-chloroaniline ($S_{p\text{-}CAN}$) is given by

$$S_{p\text{-}CAN} = \frac{[p\text{-}CAN]_{out}}{[p\text{-}CNB]_{in} - [p\text{-}CNB]_{out}} \quad (6)$$

Repeated reactions with samples from the same batch of catalyst delivered activity values that were reproducible to within ± 6 %.

Result and discussion

Catalyst characterization

Hydrogen chemisorption, BET surface areas and (surface weighted mean) Au particle size obtained by TEM (d_{TEM}) for the catalysts considered in this study are recorded in Table 1. Hydrogen uptake post-activation for all the supported Au catalysts was considerably lower (≤ 63 µmol g_{Au}^{-1}) than that obtained for conventional transition metals on oxide supports, *e.g.* Pd/Al_2O_3 (353 µmol g_{Pd}^{-1}) [33], Ni/SiO_2 (843 µmol g_{Ni}^{-1}) [55] and Ni/TiO_2 (702 µmol g_{Ni}^{-1}) [56]. Hydrogen/gold interaction is still not well understood but it appears that Au coordination number is a critical factor in determining adsorption capability [1]. While molecular hydrogen does not chemisorb on bulk Au at room temperature [57], there is evidence for dissociative chemisorption on Au films containing

Table 1

Gold particle size obtained from TEM (d_{TEM}) analysis, H_2 uptake, BET surface area and pseudo-first order p-chloronitrobenzene hydrogenation rate constant (k) obtained for oxide supported Au (1 mol %) prepared by deposition-precipitation (DP) and impregnation (IMP)

Catalyst	d_{TEM} (nm)	H_2 uptake (µmol g_{Au}^{-1})	BET area (m^2 g_{cat}^{-1})	k (h^{-1})
Au/Al_2O_3-DP	2.8	33	112	95
Au/CeO_2-DP	1.5	63	195	147
Au/Fe_2O_3-DP	2.6	21	57	89
Au/TiO_2-DP	2.4	28	48	80
Au/TiO_2-Ref	3.3	46	50	45
Au/Al_2O_3-IMP	9.0	22	161	1
Au/Fe_2O_3-IMP	3.5	27	56	35
Au/TiO_2-IMP	6.0	16	47	1

Figure 2

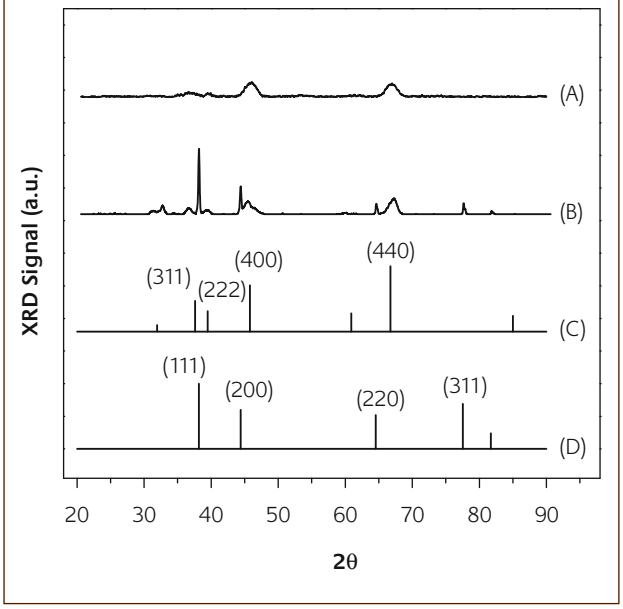

XRD patterns associated with (A) Au/Al_2O_3-DP, (B) Au/Al_2O_3-IMP and JCPDS-ICDD reference diffractograms for (C) γ-Al_2O_3 (10-0425) and (D) Au (4-0784)

Figure 3

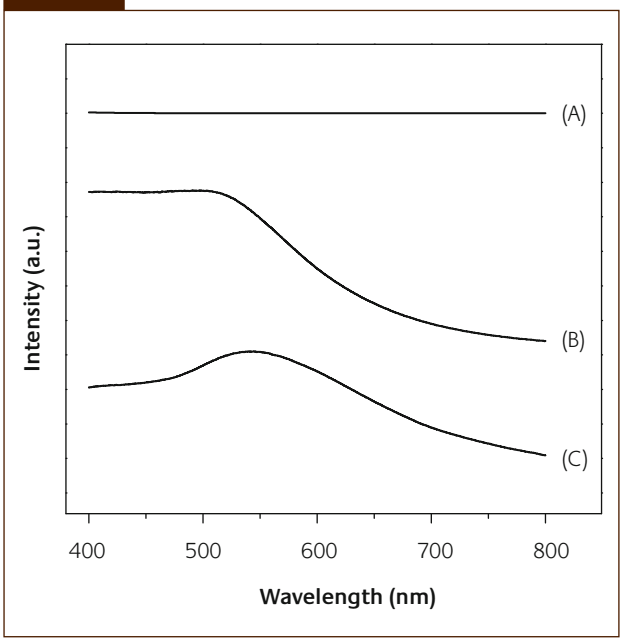

DRS UV-Vis spectra for (A) γ-Al_2O_3, (B) Au/Al_2O_3-DP and (C) Au/Al_2O_3-IMP

Figure 4

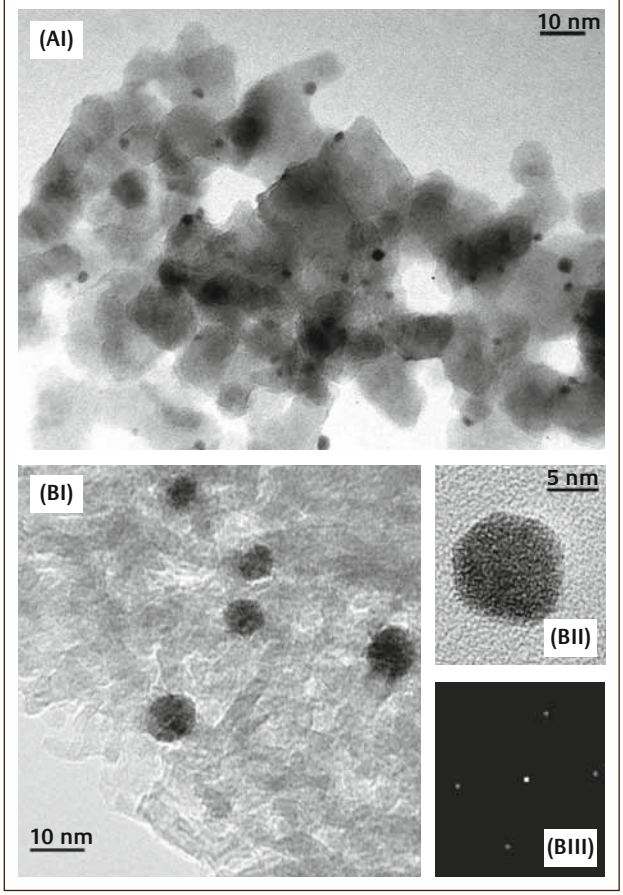

Representative TEM images of (A) Au/Al_2O_3-DP and (B) Au/Al_2O_3-IMP: (I) low magnification images; (II) high magnification image of a single Au particle (with associated diffractogram pattern (III))

defect sites [58-60]. Indeed, some consensus emerges from the literature that smaller Au particles [61-63] with a higher number of defects (steps, edges and corners) exhibit a greater facility for dissociative hydrogen uptake. X-ray diffraction analysis can provide important bulk structural characteristics. Figure 2 shows the diffraction patterns for two representative samples, *i.e.* Au/Al_2O_3-DP (profile (A)) and Au/Al_2O_3-IMP (profile (B)). The markers included illustrate the position and relative intensity of the XRD peaks for γ-Al_2O_3 (profile (C)) and cubic Au (profile (D)) taken from the JCPDS-ICDD standards (card numbers 10-0425 and 4-0784, respectively). The XRD patterns for both catalysts exhibit signals over the range 2θ = 30-70° that can be associated with the (311), (222), (400) and (440) planes of cubic γ-Al_2O_3 (see profile (C)), where the broadness of the peaks is indicative of short range order. In addition, the XRD pattern for Au/Al_2O_3-IMP (see profile (B)) also shows strong reflections at 2θ = 38.1°, 44.4°, 64.7° and 77.5° corresponding to (111), (200), (220) and (311) planes of Au metal (see profile (D)), with an extracted (from standard line broadening analysis (41)) mean Au particle size = 18 nm. In contrast, there are no distinguishable peaks characteristic of metallic gold in the Au/Al_2O_3-DP spectrum (see profile (A)), suggesting a highly dispersed Au phase. The DRS UV-Vis spectra of the alumina support, Au/Al_2O_3-DP and Au/Al_2O_3-IMP, in the range 400-800 nm, are presented in Figure 3. The spectrum for Al_2O_3 (profile (A)) is featureless, consistent with results presented elsewhere [64]. The absorption band between 500-540 nm present in the spectrum of Au/Al_2O_3-DP (profile (B)) is characteristic of metallic gold [64,65]. The signal associated with Au/Al_2O_3-IMP (profile (C)) exhibits a greater intensity with a displacement to a higher wavelength, a response that has been ascribed in the literature [66] to the presence of larger Au particles, which is in agreement with the XRD analysis.

Representative TEM images of Au/Al_2O_3-DP (AI) and Au/Al_2O_3-IMP (BI and BII) are presented in Figure 4, which show quasi-spherical Au particles dispersed on the support. The diffractogram pattern for an isolated single gold particle in the case of Au/Al_2O_3-IMP is shown in image BIII where the *d*-spacings (0.20/0.23) are consistent with the (111) and (200) planes of metallic gold (JCPDS-ICDD 4-0784), confirming precursor reduction to Au^0 post-activation, in agreement with XRD and DRS UV-Vis data. The images indicate that Au is present as smaller particles in Au/Al_2O_3-DP when compared with Au/Al_2O_3-IMP, a trend that extends to the other samples, *i.e.* for the same support, the IMP samples exhibit larger Au particles (≥ 3.5 nm, see Table 1). The sequence of increasing mean Au particle size for the samples prepared by DP, Au/CeO_2-DP < Au/TiO_2-DP < Au/Fe_2O_3-DP < Au/Al_2O_3-DP, suggests a dependency on the reducibility of the carrier, where the largest Au particle size is associated with the least reducible support (Al_2O_3). Alumina is well established as an irreducible support and an insulator material due to its wide band gap (9 eV) [67,68] whereas CeO_2, TiO_2 and Fe_2O_3 are reducible carriers with semiconductor nature (2-3 eV) [69,70]. The same trend is also in evidence for the IMP samples where the Au particle size on Al_2O_3 is appreciably higher than that for reducible TiO_2 or Fe_2O_3 (see Table 1). Our observations find some support in the literature (10) where a partial reduction of the oxide carrier has been shown to result in metal-support interactions that impact on Au dispersion. Indeed, Min *et al.* (11), using scanning tunnelling microscopy, demonstrated that reducible oxides provide more nucleation sites, leading to the formation of Au clusters with a smaller particle size.

Catalyst activity/selectivity

The gas phase hydrogenation of *p*-chloronitrobenzene over each supported Au catalyst generated *p*-chloroaniline as the sole product, *i.e.* exclusive reduction of the nitro-group with no evidence of hydrodechlorination, hydrodenitrogenation or aromatic ring reduction. It is significant that the exclusive formation of *p*-chloroaniline was a feature of each catalyst, demonstrating that the support did not influence reaction selectivity, which was governed by the Au phase. In contrast, in the hydrogenation of chloronitrobenzene over conventional transition metals, support effects have been deemed responsible for differences in selectivity. Xiong and

co-workers [71] studied the reaction of *o*-chloronitrobenzene over a series of oxide (SiO_2, ZrO_2, TiO_2 and Al_2O_3) supported Ni catalysts and attributed the highest selectivity to *o*-chloroaniline over Ni/TiO_2 to strong polarization of the N=O band induced by the oxygen vacancies of TiO_x. Han *et al.* [72] investigated the hydrogenation of *p*-chloronitrobenzene over Pt on TiO_2, γ-Al_2O_3 and ZrO_2 and associated the highest *p*-chloroaniline yield, obtained using Pt/TiO_2, with strong metal/support interactions. While Hugon *et al* [73] have recently reported that the selectivity response in the hydrogenation of 1,3-butadiene over Au supported on TiO_2, Al_2O_3, CeO_2 and ZrO_2 was independent of the nature of the support, there is evidence in the literature (6,7) of support effects in terms of hydrogenation selectivity for supported Au systems. Campo and co-workers (3) have reported that Au/CeO_2 is highly selective in the gas phase hydrogenation of crotonaldehyde to crotyl alcohol whereas Au/Nb_2O_5 is non-selective and proposed that niobia promoted the formation of non-selective Au particles with a distinct morphology. Milone *et al.* (8) reported a strong support effect with respect to C=O hydrogenation in the case of benzalacetone where electron-enriched Au particles generated via electron transfer from a reducible support (iron oxide) resulted in higher selectivities to the corresponding α,β-unsaturated alcohol. The level of reaction exclusivity reported in our study, notably the avoidance of C-Cl bond scission, is unique when compared with the catalytic batch liquid systems tested to date (30) and represents a critical advancement in the development of a sustainable continuous production of aromatic haloamines.

The activity of these catalysts was assessed by fitting the temporal x_{-NO_2} (see Figure 5) response to an empirical relationship described in detail elsewhere [33] in order to obtain a measure of initial activity. As a general observation, smaller Au particles (≤ 3.5 nm) generated higher initial activities but exhibited a temporal decline, whereas catalysts with a lower Au dispersion did not show any significant time-on-stream variation in conversion. This is demonstrated by the two representative cases presented in Figure 5: Au/Al_2O_3-IMP (d_{TEM} = 9.0 nm) delivered an invariant conversion with time-on-stream (up to 5 h), while a decline in conversion is observed for Au/Fe_2O_3-DP, which bears smaller Au particles (d_{TEM} = 2.6 nm). These results suggest a higher activity but a susceptibility to deactivation for smaller Au clusters. Metal catalyst deactivation is a feature of gas phase $-NO_2$ group reduction as a result of H_2O formation [74] and/or coke deposition [31,75-77]. The latter has been suggested as responsible for the loss of activity during hydrogenation over supported Au [78,79]. We have previously established the applicability of a pseudo-first order kinetic treatment [42,80],

$$\ln\left[\frac{1}{\left(1-(x_{-NO_2})_0\right)}\right] = k\left(\frac{n_{Au}}{F}\right) \qquad (7)$$

where n_{Au}/F has the physical meaning of contact time. The linear relationship between $\ln (1-(x_{-NO_2})_0)^{-1}$ and n_{Au}/F (forced through the origin) is shown in Figure 6, taking Au/Fe_2O_3-DP as a representative case. The resultant raw pseudo-first order rate constants (k) are given in Table 1. In order to explicitly demonstrate structure sensitivity in terms

Figure 5

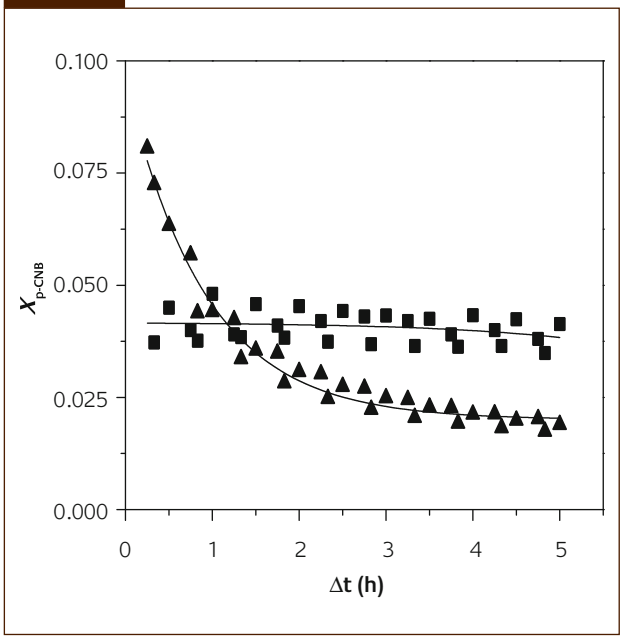

Variation of p-chloronitrobenzene fractional conversion ($x_{p\text{-}CNB}$) with time-on-stream over (▲) Au/Fe_2O_3-DP (p-CNB/Au = 463 $mol_{p\text{-}CNB}$ mol_{Au}^{-1} h^{-1}) and (■) Au/Al_2O_3-IMP (p-CNB/Au = 75 $mol_{p\text{-}CNB}$ mol_{Au}^{-1} h^{-1})

Figure 6

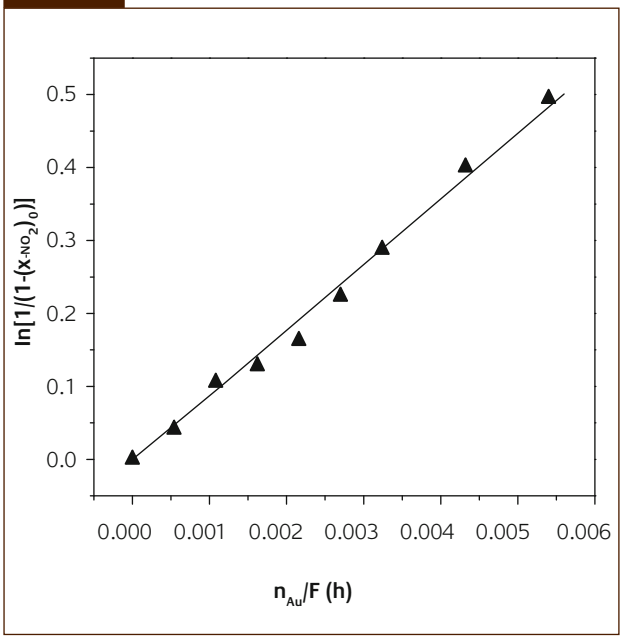

Pseudo-first order kinetic plot for the hydrogenation of p-chloronitrobenzene over Au/Fe_2O_3-DP

Figure 7

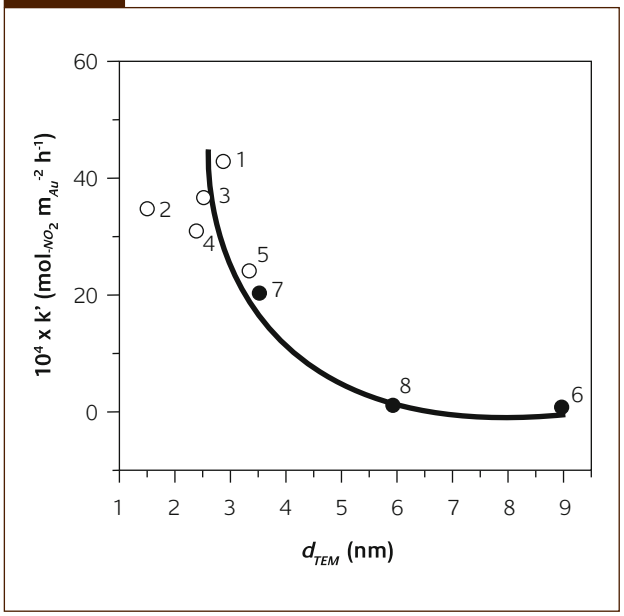

Relationship between specific rate constant (k') and Au particle size (d_{TEM}) for reaction over Au/Al_2O_3-DP (1), Au/CeO_2-DP (2), Au/Fe_2O_3-DP (3), Au/TiO_2-DP (4), Au/TiO_2-Ref (5), Au/Al_2O_3-IMP (6), Au/Fe_2O_3-IMP (7) and Au/TiO_2-IMP (8): DP catalysts represented by open circles; IMP catalysts represented by solid circles

of Au particle size, it is necessary to determine the relationship between Au size and the specific rate constant (k') in terms of the exposed Au surface area (as estimated from mean TEM particle size, see Table 1). The results are shown in Figure 7, which reveals that the catalysts prepared by DP with smaller Au particles (1.5-3.3 nm) delivered higher specific activities when compared with the IMP samples that bear larger Au particles (3.5-9.0). The observed decrease in k' with increasing Au particle size is consistent with structure sensitivity where Au particles < 4 nm are intrinsically more active for nitro-group reduction. The particle size/specific rate response for seven catalyst systems (laboratory synthesised and the World Gold Council Reference sample) fall on a common trend line. This suggests that the nature of the support does not impact significantly on hydrogenation rate, which is controlled by the Au particle size. Indeed, taking a common support (Al_2O_3, see points 1 and 6 in Figure 7) Au/Al_2O_3-DP (d_{TEM} = 2.8 nm) delivered a specific rate that was over 40 times greater than that obtained for Au/Al_2O_3-IMP (d_{TEM}=9.0nm), representing the upper and lower rate values recorded in this study. Moreover, systems with similar Au dispersion on different oxides present similar activity, as illustrated by points 3 (Au/Fe_2O_3-DP, d_{TEM} = 2.6 nm) and 4 (Au/TiO_2-DP, d_{TEM} = 2.4 nm) in Figure 7. It should be noted that Au/CeO_2-DP which presented the smallest Au particle size (1.5 nm) deviates somewhat from the general trend. We tentatively attribute this response to the small Au particle size which falls into the region (< 2 nm) where catalytic activity is severely modified by electronic and quantum size effects [81]. Indeed, the electronic character of Au can affect the catalytic response in hydrogenation reactions (13) and for particles sufficiently small (< 2 nm) a transition in the electronic state of gold from metal to non-metal has been suggested [82,83]. Moreover, Claus and co-workers [84], studying the gas phase hydrogenation of acrolein over nanosized Au/TiO_2 catalysts, associated the decrease in activity (400 → 41 mmol g_{Au}^{-1} s^{-1}) with decreasing Au particle size (2.0 → 1.4 nm) to the loss of metallic character for the smaller Au particles. In this study, we have established a significant Au particle size effect for the gas phase selective hydrogenation of *p*-chloronitrobenzene with an optimum mean Au particle size of *ca*. 3 nm that is independent of the nature of the oxide support. Future work will focus on alternative polyfunctional nitroarenes with the goal of achieving the product selectivity that we report in this study.

Conclusions

The results presented in this study support the following conclusions:

i) The continuous gas phase hydrogenation of *p*-chloronitrobenzene over Au supported on Al_2O_3, TiO_2, Fe_2O_3 and CeO_2 under mild reaction conditions (P = 1 atm; T = 423 K) results in the exclusive formation of *p*-chloroaniline.

ii) At a common Au loading (1 mol %), catalyst preparation by DP generates smaller (surface area weighted) mean Au particle sizes (≤ 3.3 nm) when compared with IMP (≥ 3.5 nm). Moreover, Au particle size was greater on the non-reducible (Al_2O_3) carrier for both preparation methods.

iii) The nature of the support does not impact directly on the rate of nitro-group reduction, which is governed by Au particle size. An increase in specific hydrogenation rate is observed with a decrease in mean Au size from 9 to 3 nm. A lower specific rate recorded for smaller particles (< 2 nm) can be attributed to a quantum size effect. A temporal loss of activity was observed for reaction over smaller Au particles whereas those catalysts with a mean particle size > 4 nm displayed a time invariant conversion.

iv) Our results can serve as a proof concept, demonstrating the feasibility of gold catalysis as a viable sustainable route for the production of aromatic amines.

Acknowledgements

The authors are grateful to Dr. W. Zhou and Mr. R. Blackley for their contribution to the TEM analysis and to Dr. C. Louis and Dr. L. Delannoy for valuable discussions. We acknowledge the World Gold Council for providing the Au/TiO_2-Ref catalyst. This work was financially supported by EPSRC through Grant 0231 110525. EPSRC support for free access to the TEM/SEM facility at the University of St Andrews is also acknowledged.

About the authors

Mark A. Keane is Professor of Chemical Engineering at Heriot-Watt University. Previously, he was Professor of Chemical & Materials Engineering, University of Kentucky (2000-2005) and Senior Lecturer in Chemical Engineering, University of Leeds (1995-2000). He is the author of over 130 papers dealing with selective hydrogenation/hydrogenolysis, kinetic modeling, catalytic growth of structured carbon and synthesis/characterization of new generation catalysts, *e.g.* carbides/nitrides and lanthanide/transition metal systems applied to clean synthesis and environmental catalysis. The development of gold catalysts falls into the latter research activity.

Fernando Cárdenas-Lizana is currently a PhD student in the Chemical Engineering Department at Heriot-Watt University. His research activities are focused on the preparation, characterization and application of supported gold-based catalysts in the continuous gas phase catalytic hydrogenation of nitroarenes as a viable, clean high throughput route to commercially important aromatic amines. He graduated as a Chemical Engineer from the University of Granada (Spain) in 2000 and obtained his MSc in "Sustainable Process Management" from Heriot-Watt University (2004).

Santiago Gómez-Quero is currently a PhD student at Heriot-Watt University. His PhD thesis deals with the catalytic hydrotreament of toxic halogenated phenols, studying fundamental aspects with applications in raw material recycle. He graduated as a Chemical Engineer from Castilla-La Mancha University (Spain) in 2005 and has a strong interest in environmental engineering, where heterogeneous catalysis has proved to be an effective tool.

Noémie Perret is currently a student at the Engineering School of Electrochemistry at Grenoble (ENSEEG-INPG). Her final dissertation research project was on oxide supported gold catalysts for selective nitro-group reduction. She will shortly begin her PhD studies in Chemical Engineering at Heriot-Watt University.

References

1 P. Claus, *Appl. Catal. A: Gen.*, 2005, **291**, 222
2 A.S.K. Hashmi, *Chem. Rev.*, 2007, **107**, 3180
3 B.C. Campo, S. Ivanova, C. Gigola, C. Petit, M.A. Volpe, *Catal. Today*, 2008, **133-135**, 661
4 T. Osaki, T. Hamada, Y. Tai, *React. Kinet. Catal. Lett.*, 2003, **78**, 217
5 G.C. Bond, C. Louis, D.T. Thompson, *Catalysis by Gold*, Imperial College Press, London, 2006
6 J.A. Lopez-Sanchez, D. Lennon, *Appl. Catal. A: Gen.*, 2005, **291**, 230
7 H. Sakurai, M. Haruta, *Appl. Catal. A: Gen.*, 1995, **127**, 93
8 C. Milone, R. Ingoglia, L. Schipilliti, C. Crisafulli, G. Neri, S. Galvagno, *J. Catal.*, 2005, **236**, 80
9 C. Milone, R. Ingoglia, A. Pistone, G. Neri, S. Galvagno, *J. Catal.*, 2004, **222**, 348.
10 J. Radnik, C. Mohr, P. Claus, *Phys. Chem. Chem. Phys.*, 2003, **5**, 172
11 B.K. Min, W.T. Wallace, D.W. Goodman, *Surf. Sci. Lett.*, 2006, **L7-L11**
12 C. Binns, *Surf. Sci. Rep.*, 2001, **44**, 1
13 C. Mohr, H. Hofmeister, P. Claus, *J. Catal.*, 2003, **213**, 86
14 B.A.A. Silberova, G. Mul, M. Makkee, J.A. Moulijn, *J. Catal.*, 2006, **243**, 171
15 D. Andreeva, V. Idakiev, T. Tabakova, L. Ilieva, P. Falaras, A. Bourlinos, A. Travlos, *Catal. Today*, 2002, **72**, 51
16 A. Sandoval, A. Gómez-Cortés, R. Zanella, G. Díaz, J.M. Saniger, *J. Mol. Catal. A: Chem.*, 2007, **278**, 200
17 V. Idakiev, T. Tabakova, Z.-Y. Yuan, B.-L. Su, *Appl. Catal. A: Gen.*, 2004, **270**, 135
18 P.N. Rylander, Catalytic Hydrogenation in Organic Synthesis. "Catalytic Dehydrohaloganation", Academic Press, Inc., New York, 1979
19 B. Chen, U. Dingerdissen, J.G.E. Krauter, H.G.J.L. Rotgerink, K. Möbus, D.J. Ostgard, P. Panster, T.H. Riermeier, S. Seebald, T. Tacke, H. Trauthwein, *Appl. Catal. A: Gen.*, 2005, **280**, 17
20 D. He, H. Shi, Y. Wu, B.-Q. Xu, *Green Chem.*, 2007, **9**, 849
21 A. Corma, P. Serna, H. García, *J. Am. Chem. Soc.*, 2007, **129**, 6358
22 A. Corma, P. Concepción, P. Serna, *Angew. Chem. Int. Ed.*, 2007, **46**, 7266
23 M. Boronat, P. Concepción, A. Corma, S. González, F. Illas, P. Serna, *J. Am. Chem. Soc.*, 2007, **129**, 16230
24 A. Corma, P. Serna, *Science*, 2006, **313**, 332
25 L. Liu, B. Qiao, Y. Ma, J. Zhang, Y. Deng, *Dalton Trans.*, 2008, 2542
26 Y. Chen, J. Qiu, X. Wang, J. Xiu, *J. Catal.*, 2006, **242**, 227
27 G. Konnecker, A. Boehncke, S. Schmidt, *Fresenius Environ. Bull.*, 2003, **12**, 589
28 A. Boehnecke, J. Kielhorn, G. Konnecker, C. Pohlenz-Michel, I. Mangelsdorf, CICADS Report 48, W.H.O., Geneva, 2003, p. 78

29 K.R. Westerterp, E.J. Molga, K.B. van Gelder, *Chem. Eng. Process.*, 1997, **36**, 17

30 X.D. Wang, M.H. Liang, J.L. Zhang, Y. Wang, *Curr. Org. Chem.*, 2007, **11**, 299

31 V. Vishwanathan, V. Jayasri, P.M. Basha, N. Mahata, L.M. Sikhwivhilu, N.J. Coville, *Catal. Commun.*, 2008, **9**, 453.

32 V. Kratky, M. Kralik, M. Mecarova, M. Stolcova, L. Zalibera, M. Hronec, *Appl. Catal. A: Gen.*, 2002, **235**, 225

33 F. Cárdenas-Lizana, S. Gómez-Quero, M.A. Keane, *Catal. Commun.*, 2008, **9**, 475

34 C. Xi, H. Cheng, J. Hao, S. Cai, F. Zhao, *J. Mol. Catal. A: Chem.*, 2008, **282**, 80

35 Y.-Z. Chen, Y.-C. Chen, *Appl. Catal. A: Gen.*, 1994, **115**, 45

36 Y.-C. Liu, C.-Y. Huang, Y.-W. Chen, *Ind. Eng. Chem. Res.*, 2006, **45**, 62

37 Y.-C. Liu, Y.-W. Chen, *Ind. Eng. Chem. Res.*, 2006, **45**, 2973

38 Z. Yu, S. Liao, Y. Xu, B. Yang, D. Yu, *J. Mol. Catal. A: Chem.*, 1997, **120**, 247

39 B. Coq, A. Tijani, F. Figuéras, *J. Mol. Catal.*, 1991, **68**, 331

40 V.L. Khilnani, S.B. Chandalia, *Org. Proc. Res. Dev.*, 2001, **5**, 257

41 F. Cárdenas-Lizana, S. Gómez-Quero, M.A. Keane, *Appl. Catal. A: Gen.*, 2008, **334**, 199

42 F. Cárdenas-Lizana, S. Gómez-Quero, M.A. Keane, *ChemSusChem*, 2008, **1**, 215

43 G. Neri, A.M. Visco, S. Galvagno, A. Donato, M. Panzalorto, *Thermochim. Acta*, 1999, **329**, 39

44 F.E. Wagner, S. Galvagno, C. Milone, A.M. Visco, L. Stievano, S. Calogero, *J. Chem. Soc. Faraday Trans.*, 1997, **93**, 3403

45 D. Andreeva, V. Idakiev, T. Tabakova, A. Andreev, R. Giovanoli, *Appl. Catal. A: Gen.*, 1996, **134**, 275

46 G.C. Bond, D.T. Thompson, *Cat. Rev.-Sci. Eng.*, 1999, **41**, 319

47 M. Haruta, *Catal. Today*, 1997, **36**, 153

48 M. Khoudiakov, M.C. Gupta, S. Deevi, *Appl. Catal. A: Gen.*, 2005, **291**, 151

49 M. Haruta, S. Tsubota, T. Kobayashi, H. Kageyama, M.J. Genet, B. Delmon, *J. Catal.*, 1993, **144**, 175

50 S. Tsubota, A. Yamaguchi, M. Daté, M. Haruta, "*Characterization of Reference Gold Catalysts" in GOLD2003, the 3rd International Conference on Gold Science, Technology and its Applications, September-October, 2003, Vancouver, Canada*

51 L. Delannoy, N. Weiher, N. Tsapatsaris, A.M. Beesley, L. Nchari, S.L.M. Schroeder, C. Louis, *Top. Catal.*, 2007, **44**, 263

52 G. Tavoularis, M.A. Keane, *J. Chem. Technol. Biotechnol.*, 1999, **74**, 60

53 C.M. Van Den Bleek, K. Van Der Wiele, P.J. Van Der Berg, *Chem. Eng. Sci.*, 1969, **24**, 681

54 G. Yuan, M.A. Keane, *Chem. Eng. Sci.*, 2003, **58**, 257

55 G. Yuan, J.L. Lopez, C. Louis, L. Delannoy, M.A Keane, *Catal. Commun.*, 2005, **6**, 555

56 G. Yuan, C. Louis, L. Delannoy, M.A. Keane, *J. Catal.*, 2007, **247**, 256

57 A.G. Sault, R.J. Madix, C.T. Campbell, *Surf. Sci.*, 1986, **169**, 347

58 L. Stobiński, L. Zommer, R. Duś, *Appl. Surf. Sci.*, 1999, **141**, 319

59 M. Okada, M. Nakamura, K. Moritani, T. Kasai, *Surf. Sci.*, 2003, **523**, 218

60 M. Okada, S. Ogura, W.A. Diño, M. Wilde, K. Fukutani, T. Kasai, *Appl. Catal. A: Gen.*, 2005, **291**, 55

61 M. Okumura, T. Akita, M. Haruta, *Catal. Today*, 2002, **74**, 265

62 R. Zanella, C. Louis, S. Giorgio, R. Touroude, *J. Catal.*, 2004, **223**, 328

63 J. Stoczyński, R. Grabowski, A. Koztowska, P. Olszewski, J. Stoch, J. Skrzypek, M. Lachowska, *Appl. Catal. A: Gen.*, 2004, **278**, 11

64 A.C. Gluhoi, X. Tang, P. Marginean, B.E. Nieuwenhuys, *Top. Catal.*, 2006, **39**, 101

65 T.-H. Kim, D.-W. Kim, J.-M. Lee, Y.-G. Lee, S.-G. Oh, *Mater. Res. Bull.*, 2008, **43**, 1126

66 X. Hu, D.J. Blackwood, *J. Electroceram.*, 2006, **16**, 593

67 C. Karunakaran, P. Anilkumar, *J. Mol. Catal. A: Chem.*, 2007, **265**, 153

68 C. Karunakaran, P. Anilkumar, *Sol. Energy Mater. Sol. Cells*, 2008, **92**, 490

69 C. Karunakaran, R. Dhanalakshmi, S. Karuthapandian, *J. Photochem. Photobiol., A* 2005, **170**, 233

70 C. Sol, R.J.D. Tilley, *J. Mater. Chem.*, 2001, **11**, 815

71 J. Xiong, J.X. Chen, J.Y. Zhang, *Catal. Commun.*, 2007, **8**, 345

72 X.-X. Han, R.-X. Zhou, G.-H. Lai, X.-M. Zheng, *Catal. Today*, 2004, **93-95**, 433

73 A. Hugon, L. Delannoy, C. Louis, *Gold Bulletin*, 2008, **41**, 127

74 P. Sangeetha, P. Seetharamulu, K. Shanthi, S. Narayanan, K.S. Rama Raob, *J. Mol. Catal. A: Chem.*, 2007, **273**, 244

75 S. Diao, W. Qian, G. Luo, F. Wei, Y. Wang, *Appl. Catal. A: Gen.*, 2005, **286**, 30

76 L. Petrov, K. Kumbilieva, N. Kirkov, *Appl. Catal.*, 1990, **59**, 31

77 E. Klemm, B. Amon, H. Redlingshöfer, E. Dieterich, G. Emig, *Chem. Eng. Sci.*, 2001, **56**, 1347

78 Y. Azizi, C. Petit, V. Pitchon, *J. Catal.*, 2008, **256**, 338

79 B. Pawelec, A.M. Venezia, V. La Parola, S. Thomas, J.L.G. Fierro, *Appl. Catal. A: Gen.*, 2005, **283**, 165

80 F. Cárdenas-Lizana, S. Gómez-Quero, M.A. Keane, *Catal. Lett.*, 2009, **127**, 25

81 M. Valden, X. Lai, D.W. Goodman, *Science*, 1998, **281**, 1647

82 K. Okazaki, S. Ichikawa, Y. Maeda, M. Haruta, M. Kohyama, *Appl. Catal. A: Gen.*, 2005, **291**, 45

83 C.P. Vinod, G.U. Kulkarni, C.N.R. Rao, *Chem. Phys. Lett.*, 1998, **289**, 329

84 P. Claus, A. Brückner, C. Mohr, H. Hofmeister, *J. Am. Chem. Soc.*, 2000, **122**, 11430